

Nonlinear stability of convective flow between heated vertical planes

P.G. DANIELS¹ and M. WEINSTEIN²

¹Department of Mathematics, City University, Northampton Square, London EC1V 0HB, UK

²Raphael, P.O. Box 2250, Haifa 31021, Israel

Received 13 December 1988; accepted in revised form 24 April 1989

Abstract. A weakly nonlinear stability analysis is described for the buoyancy-driven flow between infinite vertical planes that are subject to a constant vertical temperature gradient and a constant horizontal temperature difference. For sufficiently high values of a Rayleigh number based on the vertical temperature gradient and gap width, and for large Prandtl numbers, the critical two-dimensional mode of instability occurs as stationary convection. A nonlinear amplitude equation governing the spatial and temporal development near the critical point is determined.

1. Introduction

The buoyancy-driven flow between vertical planes that are maintained at different temperatures has been widely studied because of its relevance in a variety of geophysical, astrophysical and technological areas. Thermal properties of the flow are of importance in the context of wall and window insulation and also in cooling systems for nuclear reactors. A more recent application is to high-speed microcomputers where immersion-cooling techniques are being developed to allow the close packing of electrical components on circuit boards. Non-electrically conducting fluids that are used generally have high Prandtl numbers.

A horizontal temperature difference maintained across the gap between two vertical planes produces an antisymmetric vertical flow up on the hot side and down on the cold side. This flow is modified if a vertical temperature gradient is also present and an exact solution of the Boussinesq equations for this situation has been given by Elder [1]. The appropriate parameter that defines the base flow is a vertical Rayleigh number

$$R = \alpha^* g^* \Delta T_v^* l^{*3} / \kappa \nu = 4\gamma^4, \quad (1)$$

where α^* is the coefficient of thermal expansion, g^* is the acceleration due to gravity, κ is the thermal diffusivity and ν is the kinematic viscosity. The vertical temperature gradient is $\Delta T_v^* / l^*$ where l^* is the gap width between the planes.

The linear stability of this flow has been thoroughly examined by Bergholz [2] and when the Prandtl number of the fluid, $\sigma = \nu / \kappa$, is infinite and $\gamma > \gamma_c$ where $\gamma_c \approx 6.3$ (see Daniels [3]) there is a stationary mode of instability for horizontal Rayleigh numbers

$$A = \alpha^* g^* \Delta T_h^* l^{*3} / \kappa \nu \quad (2)$$

greater than a certain critical value $A_c(\gamma)$. Travelling modes of instability have critical Rayleigh numbers A proportional to $\sigma^{1/2}$ as $\sigma \rightarrow \infty$ (see Gill and Kirkham [4]) and are therefore of less significance at large Prandtl numbers. The asymptotic form as $\gamma \rightarrow \infty$ of the stationary mode of instability has been discussed by Daniels [5].

The governing equations, boundary conditions and base flow are described in Section 2. In Section 3 a weakly nonlinear analysis is developed to describe the finite-amplitude solutions that evolve near A_c . The results of this analysis are discussed in Section 4, partly in relation to calculations and observations of secondary motion in vertical-slot flows. One reason for studying the exact solution referred to above is that it approximates the type of flow that develops at mid-height in a vertical slot with constant temperature sidewalls and closed ends, a classical problem in thermal convection widely considered experimentally, theoretically and numerically (see [3]). There the vertical temperature gradient is induced in the interior of the slot by the presence of the end-walls but at mid-height detailed comparisons of the exact solution with experimental results and theoretical results based on a boundary-layer approximation are very favourable (see [1], [3]).

2. Governing equations and base flow

A fluid fills the gap $-\infty < z^* < \infty$ between parallel planes $x^* = \pm \frac{1}{2}l^*$ which are maintained at temperatures

$$T^* = T_0^* \pm \frac{1}{2} \Delta T_h^* + \Delta T_v^* z^*/l^* \quad (x^* = \pm \frac{1}{2}l^*), \quad (3)$$

where T_0^* is a suitable reference value. In the Boussinesq approximation the equations that govern two-dimensional flow in the limit of infinite Prandtl number may be written

$$\nabla^4 \psi - A \frac{\partial T}{\partial x} = 0, \quad (4)$$

$$\nabla^2 T = \frac{\partial T}{\partial t} + \frac{\partial(T, \psi)}{\partial(x, z)}. \quad (5)$$

Here the co-ordinates x, z , time t and stream function ψ are made non-dimensional by the quantities l^* , l^{*2}/κ and κ respectively, while T is the non-dimensional temperature perturbation defined by

$$T^* = T_0^* + \Delta T_h^* T. \quad (6)$$

The boundary conditions at the vertical planes are

$$\psi = \frac{\partial \psi}{\partial x} = 0, \quad T = \beta z \pm \frac{1}{2} \quad \text{on } x = \pm \frac{1}{2}, \quad (7)$$

where $\beta = \Delta T_v^*/\Delta T_h^*$.

The exact solution of (4), (5) and (7) of interest here is the bi-directional flow

$$\psi = \psi_0 = A\Phi(x), \quad T = T_0 = \beta z + \Theta(x). \quad (8)$$

The functions Φ and Θ satisfy

$$\Phi^{IV} - \Theta' = 0, \quad \Theta'' + 4\gamma^4 \Phi' = 0, \quad (9)$$

with boundary conditions

$$\Phi = \Phi' = 0, \quad \Theta = \pm \frac{1}{2} \quad \text{on } x = \pm \frac{1}{2}, \quad (10)$$

and so are functions of the single parameter γ defined by

$$\gamma^4 = \frac{1}{4} A\beta \quad (11)$$

and equivalent to (1) above. The required solutions are

$$\begin{aligned} \Phi = & (\sinh \gamma + \sin \gamma + \cosh x_+ \sin x_- + \sinh x_- \cos x_+ - \sinh x_+ \cos x_- \\ & - \cosh x_- \sin x_+)/8\gamma^3 d, \end{aligned} \quad (12)$$

$$\Theta = (\cosh x_+ \cos x_- - \cosh x_- \cos x_+)/2d, \quad (13)$$

where $x_{\pm} = \gamma(x \pm \frac{1}{2})$ and $d = \cosh \gamma - \cos \gamma$.

3. Stability analysis

Perturbations $\tilde{\psi}, \tilde{T}$ of the base flow such that

$$\psi = A(\Phi(x) + \tilde{\psi}), \quad T = \beta z + \Theta(x) + \tilde{T}, \quad (14)$$

are governed by the system

$$\nabla^4 \tilde{\psi} - \frac{\partial \tilde{T}}{\partial x} = 0, \quad (15)$$

$$\nabla^2 \tilde{T} + 4\gamma^4 \frac{\partial \tilde{\psi}}{\partial x} = \frac{\partial \tilde{T}}{\partial t} + A \frac{\partial(\tilde{T}, \tilde{\psi})}{\partial(x, z)}, \quad (16)$$

$$\tilde{\psi} = \frac{\partial \tilde{\psi}}{\partial x} = \tilde{T} = 0 \quad (x = \pm \frac{1}{2}). \quad (17)$$

Let

$$A = A_c + \varepsilon, \quad (18)$$

where $\varepsilon \ll A_c$ and consider solutions

$$\begin{aligned} \tilde{\psi} = & \varepsilon^{1/2} \psi_1 + \varepsilon \psi_2 + \varepsilon^{3/2} \psi_3 + \dots, \\ \tilde{T} = & \varepsilon^{1/2} T_1 + \varepsilon T_2 + \varepsilon^{3/2} T_3 + \dots, \end{aligned} \quad (19)$$

where ψ_i and T_i are functions of x, z and appropriate long length and time scales Z and τ defined by

$$z = \varepsilon^{-1/2} Z, \quad t = \varepsilon^{-1} \tau. \quad (20)$$

Substitution of (19) into (15)–(17) gives, at order $\epsilon^{1/2}$,

$$\nabla^4 \psi_1 - \frac{\partial T_1}{\partial x} = 0, \tag{21}$$

$$\nabla^2 T_1 + 4\gamma^4 \frac{\partial \psi_1}{\partial x} = A_c \left(\Theta' \frac{\partial \psi_1}{\partial z} - \Phi' \frac{\partial T_1}{\partial z} \right), \tag{22}$$

$$\psi_1 = \frac{\partial \psi_1}{\partial x} = T_1 = 0 \quad (x = \pm \frac{1}{2}). \tag{23}$$

This is equivalent to the linear stability problem examined by Bergholz [2] and has a solution

$$\psi_1 = B(Z, \tau) e^{i\alpha_c z} f(x) + B^*(Z, \tau) e^{-i\alpha_c z} f^*(x), \tag{24}$$

$$T_1 = B(Z, \tau) e^{i\alpha_c z} g(x) + B^*(Z, \tau) e^{-i\alpha_c z} g^*(x), \tag{25}$$

where * now denotes complex conjugate,

$$f^{IV} - 2\alpha_c^2 f'' + \alpha_c^4 f - g' = 0, \tag{26}$$

$$g'' - \alpha_c^2 g + 4\gamma^4 f' = i\alpha_c A_c (\Theta' f - \Phi' g), \tag{27}$$

$$f = f' = g = 0 \quad (x = \pm \frac{1}{2}), \tag{28}$$

and B is a complex amplitude function. The wavenumber α_c is the critical wavenumber associated with the minimum point A_c of the neutral curve, as determined in [2]. Table 1 shows values of α_c and A_c obtained from the solution of (26)–(28) in the region $-\frac{1}{2} \leq x \leq 0$ by use of a fourth order Runge–Kutta scheme. Symmetry properties of (26)–(28) allow the solution to be expressed as

$$f = f_o + if_e, \quad g = g_e + ig_o, \tag{29}$$

Table 1. Critical Rayleigh numbers and wavenumbers

γ	A_c	α_c
6.7	499242.0	2.2804
7	303355.4	2.83
7.5	235511.3	3.4276
8	237826.5	3.8448
9	317211.7	4.38
10	471451.2	4.6988
10.5	577965.3	4.8061
11	702358.9	4.89
11.5	839245.2	4.9639
12	983267.6	5.0541
12.5	1133393.5	5.1643
13	1292823.0	5.29
14	1656755.6	5.5395
15	2098858.0	5.7751
16	2626830.5	5.9962
17	3243503.6	6.2106

where f_o, g_o, f_e and g_e are odd and even real functions of x respectively (see Vest and Arpaci [6]). Six lineary independent real solution vectors

$$(f_o, f'_o, f''_o, f'''_o, f_e, f'_e, f''_e, f'''_e, g_e, g'_e, g_o, g'_o) \tag{30}$$

are computed from $x = -\frac{1}{2}$ to $x = 0$. At $x = 0$ application of the symmetry conditions

$$f_o = f''_o = f'_e = f'''_e = g'_e = g_o = 0 \tag{31}$$

yields a determinant which must vanish at points on the neutral stability curve. The zeros of the determinant were located by iterative adjustment of A at fixed values of α using Newton's method in the generalized version of (26)–(28). The critical points given in Table 1 are in good agreement with those obtained by Bergholz [2] using a Galerkin method. Typical profiles are shown in Fig. 1 and the solution is normalized so that $g_e(0) = 1$.

At order ε ,

$$\nabla^4 \psi_2 - \frac{\partial T_2}{\partial x} = -4 \left(\frac{\partial^2}{\partial x^2} + \frac{\partial^2}{\partial z^2} \right) \frac{\partial^2 \psi_1}{\partial z \partial Z}, \tag{32}$$

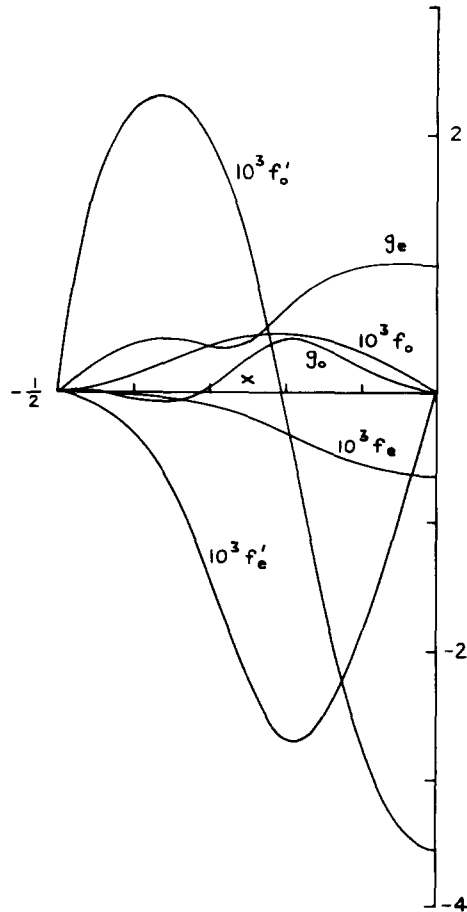


Fig. 1. Eigenfunctions of the linear stability problem for $\gamma = 9$.

$$\nabla^2 T_2 + 4\gamma^4 \frac{\partial \psi_2}{\partial x} - A_c \left(\Theta' \frac{\partial \psi_2}{\partial z} - \Phi' \frac{\partial T_2}{\partial z} \right) = -2 \frac{\partial^2 T_1}{\partial z \partial Z} + A_c \left(\Theta' \frac{\partial \psi_1}{\partial Z} - \Phi' \frac{\partial T_1}{\partial Z} + \frac{\partial \psi_1}{\partial z} \frac{\partial T_1}{\partial x} - \frac{\partial \psi_1}{\partial x} \frac{\partial T_1}{\partial z} \right), \quad (33)$$

$$\psi_2 = \frac{\partial \psi_2}{\partial x} = T_2 = 0 \quad (x = \pm \frac{1}{2}), \quad (34)$$

with solutions

$$\psi_2 = \frac{\partial B}{\partial Z} e^{i\alpha_c z} \hat{f}(x) + \frac{\partial B^*}{\partial Z} e^{-i\alpha_c z} \hat{f}^*(x) + |B|^2 \bar{f}(x) + B^2 e^{2i\alpha_c z} \tilde{f}(x) + B^{*2} e^{-2i\alpha_c z} \tilde{f}^*(x), \quad (35)$$

$$T_2 = \frac{\partial B}{\partial Z} e^{i\alpha_c z} \hat{g}(x) + \frac{\partial B^*}{\partial Z} e^{-i\alpha_c z} \hat{g}^*(x) + |B|^2 \bar{g}(x) + B^2 e^{2i\alpha_c z} \tilde{g}(x) + B^{*2} e^{-2i\alpha_c z} \tilde{g}^*(x). \quad (36)$$

Here the omission of possible eigensolutions proportional to ψ_1 and T_1 does not affect the amplitude equation for B to be determined below. The equations for \hat{f} , \hat{g} , \bar{f} , \bar{g} and \tilde{f} , \tilde{g} are

$$\hat{f}^{IV} - 2\alpha_c^2 \hat{f}'' + \alpha_c^4 \hat{f} - \hat{g}' = 4i\alpha_c(\alpha_c^2 f - f'') = \chi_1, \quad (37)$$

$$\hat{g}'' - \alpha_c^2 \hat{g} + 4\gamma^4 \hat{f}' - i\alpha_c A_c(\Theta' \hat{f} - \Phi' \hat{g}) = -2i\alpha_c g + A_c(\Theta' f - \Phi' g) = \chi_2,$$

$$\bar{f}^{IV} - \bar{g}' = 0, \quad (38)$$

$$\bar{g}'' + 4\gamma^4 \bar{f}' = i\alpha_c A_c(fg^{*'} - f^*g' + f'g^* - f^{*'}g),$$

$$\tilde{f}^{IV} - 8\alpha_c^2 \tilde{f}'' + 16\alpha_c^4 \tilde{f} - \tilde{g}' = 0, \quad (39)$$

$$\tilde{g}'' - 4\alpha_c^2 \tilde{g} + 4\gamma^4 \tilde{f}' - 2i\alpha_c A_c(\Theta' \tilde{f} - \Phi' \tilde{g}) = i\alpha_c A_c(fg' - f'g).$$

Again symmetry properties may be used to advantage, giving

$$\hat{f} = \hat{f}_e - i\hat{f}_o, \quad \hat{g} = \hat{g}_o - i\hat{g}_e, \quad (40)$$

$$\bar{f} = \bar{f}_e, \quad \bar{g} = \bar{g}_o, \quad (41)$$

$$\tilde{f} = \tilde{f}_e + i\tilde{f}_o, \quad \tilde{g} = \tilde{g}_o + i\tilde{g}_e. \quad (42)$$

The resulting sets of real equations are solved in the region $-\frac{1}{2} \leq x \leq 0$ using the Runge-Kutta method and the appropriate symmetry conditions at $x = 0$.

Solutions for \hat{f} and \hat{g} may actually be expressed as

$$\hat{f} = -i \left. \frac{\partial f}{\partial \alpha} \right|_{\alpha_c}, \quad \hat{g} = -i \left. \frac{\partial g}{\partial \alpha} \right|_{\alpha_c}, \quad (43)$$

where on the right-hand sides f and g must be viewed as functions of both x and α at points on the neutral stability curve $A = A(\alpha)$ and the derivatives are then evaluated at the critical point where $dA/d\alpha = 0$. The existence of this solution for \hat{f} and \hat{g} , despite forcing of the basic linear system is equivalent, in the numerical solution, to the fact that one row of the matrix equation obtained from satisfaction of the six boundary conditions at $x = 0$ is

automatically satisfied. Thus one of the six arbitrary real constants remains undetermined, equivalent to the existence of the basic eigenfunctions f and g , while the other five can be consistently determined even though the determinant of the coefficient matrix, which is identical to that of the basic linear system, is zero. Runge–Kutta computations of \hat{f} , \bar{g} , \tilde{f} and \tilde{g} are carried out in a straightforward manner.

The solution for \hat{f} , \hat{g} exists because the adjoint condition

$$\int_{-\frac{1}{2}}^{\frac{1}{2}} (\chi_1 F + \chi_2 G) dx = 0 \tag{44}$$

associated with the forced system (37) is automatically satisfied. The adjoint functions F and G which satisfy

$$F^{IV} - 2\alpha_c^2 F'' + \alpha_c^4 F - 4\gamma^4 G' - i\alpha_c A_c \Theta' G = 0, \tag{45}$$

$$G'' - \alpha_c^2 G + F' + i\alpha_c A_c \Phi' G = 0, \tag{46}$$

$$F = F' = G = 0 \quad (x = \pm \frac{1}{2}), \tag{47}$$

can be expressed in real and imaginary parts as

$$F = F_o + iF_e, \quad G = G_e + iG_o. \tag{48}$$

In the Runge–Kutta solution for F and G the determinant of the coefficient matrix obtained from the six real boundary conditions at $x = 0$ must vanish, providing an additional check on the computation of the neutral curve, α_c and A_c .

At order $\epsilon^{3/2}$ the solutions for ψ_3 and T_3 involve terms proportional to $e^{i\alpha_c z}$ which again satisfy equations of the form (37) but with

$$\chi_1 = \{4i\alpha_c(\alpha_c^2 \hat{f} - \hat{f}'') + 2(3\alpha_c^2 f - f'')\} \frac{\partial^2 B}{\partial Z^2}, \tag{49}$$

$$\begin{aligned} \chi_2 = \{g\} \frac{\partial B}{\partial \tau} + \{A_c(\Theta' \hat{f} - \Phi' \hat{g}) - 2i\alpha_c \hat{g} - g\} \frac{\partial^2 B}{\partial Z^2} \\ + \{i\alpha_c A_c(f\bar{g}' - \bar{f}'g + \tilde{f}'g^* - f^*\tilde{g}' + 2\tilde{f}g^{*'} - 2f^{*'}\tilde{g})\} B|B|^2 \\ + \{i\alpha_c(\Theta' f - \Phi' g)\} B. \end{aligned} \tag{50}$$

The adjoint condition (44) now implies that consistent solutions exist only if

$$a_1 \frac{\partial B}{\partial \tau} = a_2 \frac{\partial^2 B}{\partial Z^2} + a_3 B - a_4 B|B|^2, \tag{51}$$

where

$$a_1 = \int_{-\frac{1}{2}}^0 \{g_o G_o - g_e G_e\} dx, \tag{52}$$

$$a_2 = \int_{-\frac{1}{2}}^0 \{ (2\alpha_c \hat{g}_e - g_e + A_c [\Theta' \hat{f}_e - \Phi' \hat{g}_o]) G_e + (2\alpha_c \hat{g}_o + g_o + A_c [\Phi' \hat{g}_e - \Theta' \hat{f}_o]) G_o + (4\alpha_c \hat{f}_o'' - 4\alpha_c^3 \hat{f}_o + 6\alpha_c^2 f_o - 2f_o'') F_o + (4\alpha_c \hat{f}_e'' - 4\alpha_c^3 \hat{f}_e - 6\alpha_c^2 f_e + 2f_e'') F_e \} dx, \quad (53)$$

$$a_3 = \alpha_c \int_{-\frac{1}{2}}^0 \{ (\Phi' g_o - \Theta' f_e) G_e + (\Phi' g_e - \Theta' f_o) G_o \} dx, \quad (54)$$

$$a_4 = \alpha_c A_c \int_{-\frac{1}{2}}^0 \{ [2(\tilde{f}_o g_e' - \tilde{f}_e g_o' + f_e \tilde{g}_o - f_o \tilde{g}_e) + f_e \bar{g}_o' - \bar{f}_e g_o - \tilde{f}_e g_o + \tilde{f}_o g_e - f_o \tilde{g}_e' + f_e \tilde{g}_o'] G_e + [2(\tilde{f}_e g_e' + \tilde{f}_o g_o' - f_o \tilde{g}_o - f_e \tilde{g}_e) + f_o \bar{g}_e' - \bar{f}_e g_e - f_o \tilde{g}_o' - f_e \tilde{g}_e' + \tilde{f}_e g_e + \tilde{f}_o g_o] G_o \} dx. \quad (55)$$

These integrals were calculated using Simpson's rule. Most Runge-Kutta computations were carried out with 80 steps across the region $-\frac{1}{2} \leq x \leq 0$ for the basic linear and adjoint functions and 40 for the higher-order functions. Checks with double step sizes were carried out in several cases and indicated excellent accuracy for the finer grid.

4. Results and discussion

The amplitude coefficients (52)–(55) are shown as functions of the base-flow parameter γ in Fig. 2. There is clearly a singular behaviour near γ_c associated with the corresponding behaviour of A_c . As γ increases from γ_c the base flow develops regions of weak flow reversal near $x=0$ ($\gamma > 7.85$) and the nonlinear coefficient a_4/a_3 decreases initially. It becomes

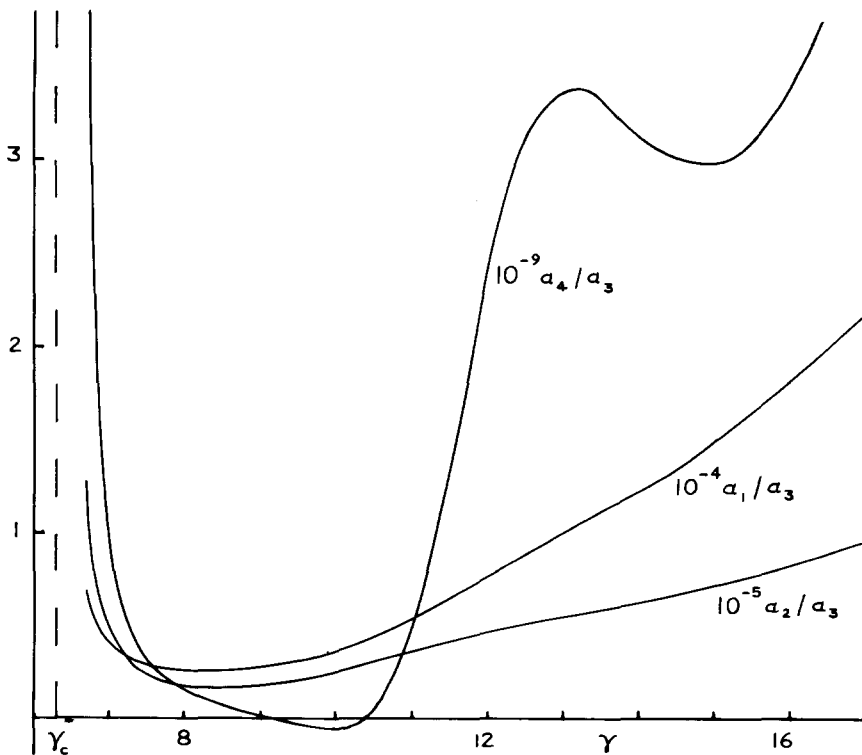


Fig. 2. Amplitude equation coefficients a_1/a_3 , a_2/a_3 , a_4/a_3 .

slightly negative near $\gamma = 10$, indicating a small region of subcritical instability there, but rises again to higher values beyond that. Thus in most circumstances a stable finite-amplitude motion exists as A increases above A_c , and Fig. 3 shows a typical streamline pattern, accurate to order $\varepsilon^{1/2}$, for the case where $\gamma = 11.5$. Here $B = (a_3/a_4)^{1/2}$ is taken to be the constant steady-state value corresponding to the periodic solution of (51) for which the disturbance amplitude is maximum i.e. for which the adjustment to the critical wavelength represented by the spatial modulation term $\partial^2 B / \partial Z^2$ is zero. Note that a large value of ε must be selected in order for the disturbance flow to have a visible impact on the base state. This merely reflects the (typically) large numerical value of A_c so that in Fig. 3 even with $\varepsilon = 5 \times 10^4$ the perturbation to A_c in (18), which corresponds to $A/A_c \approx 1.06$, represents only a 6% change in the Rayleigh number. For the selected value of ε the main features of the overall motion in Fig. 3 are large counter-clockwise rolls separated by weaker regions of clockwise rotation. Similar behaviour has been observed in both numerical work ([7], [8]) and experiments ([1], [6], [9]). Recent experimental work by Simpkins and Godreau [10] using a large-Prandtl-number silicone oil shows a streamline pattern very similar to that of Fig. 3, including both the separate co-rotating eddies within each main roll and the weaker counter-rotating rolls referred to as ‘tertiary’ motion by Elder [1]. Also, both experimental and numerical work has shown that the main counter-clockwise rolls slant up towards the hotter wall at the onset of motion, in the manner depicted in Fig. 3.

At large values of γ the magnitudes of the amplitude coefficients can be estimated from scalings associated with the development of buoyancy layers near each vertical plane where $x \pm \frac{1}{2} = O(\gamma^{-1})$. Here $\Phi = O(\gamma^{-3})$ and $\Theta = O(1)$ while in the intervening core region $\Phi \approx \frac{1}{8}\gamma^{-3}$ and $\Theta \approx 0$. The linear stability problem then has

$$\alpha_c \sim 1.6\gamma^{1/2}, \quad A_c \sim 153\gamma^{7/2} \quad (\gamma \rightarrow \infty), \tag{56}$$

with $f = O(\gamma^{-3})$ and $g = O(1)$ in buoyancy layers and core (see Daniels [5]). The corresponding scalings for the higher-order terms involved in the nonlinear analysis of Section 3 then suggest that

$$a_1/a_3 = O(\gamma^{5/2}), \quad a_2/a_3 = O(\gamma^{5/2}), \quad a_4/a_3 = O(\gamma^{7/2}), \tag{57}$$

as $\gamma \rightarrow \infty$.

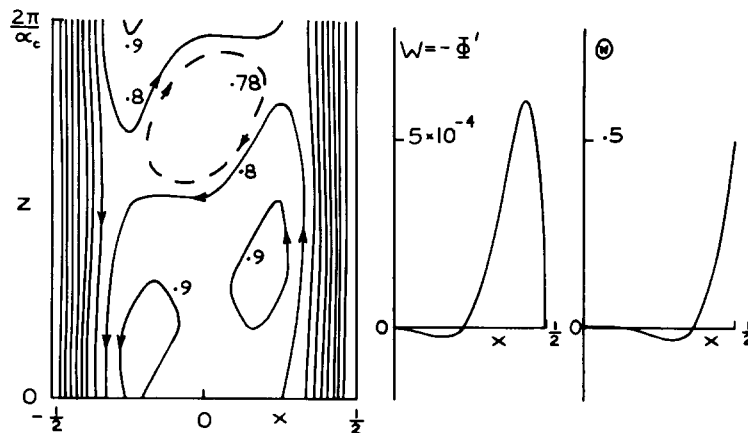


Fig. 3. Streamlines $10^4\psi/A$ predicted by the present theory for $\gamma = 11.5$ ($A_c = 839245$, $\alpha_c = 4.9639$) and $\varepsilon = 5 \times 10^4$ ($A = 889245$). Base profiles of velocity and temperature are also shown.

References

1. J.W. Elder, Laminar free convection in a vertical slot, *J. Fluid Mech.* 23 (1965) 77–98.
2. R.F. Bergholz, Instability of steady natural convection in a vertical fluid layer, *J. Fluid Mech.* 84 (1978) 743–768.
3. P.G. Daniels, Convection in a vertical slot, *J. Fluid Mech.* 176 (1987) 419–441.
4. A.E. Gill and C.C. Kirkham, A note on the stability of convection in a vertical slot, *J. Fluid Mech.* 42 (1970) 125–127.
5. P.G. Daniels, Stationary instability of the buoyancy-layer flow between heated vertical planes, *Proc. R. Soc. A* 401 (1985) 145–161.
6. C.M. Vest and V.S. Arpaci, Stability of natural convection in a vertical slot, *J. Fluid Mech.* 36 (1969) 1–15.
7. G. de Vahl Davis and G.D. Mallinson, A note on natural convection in a vertical slot, *J. Fluid Mech.* 72 (1975) 87–93.
8. Y. Lee and S.A. Korpela, Multi-cellular convection in a vertical slot, *J. Fluid Mech.* 126 (1983) 91–121.
9. N. Seki, S. Fukusako and H.J. Inaba, Visual observations of natural convection flow in a narrow vertical cavity, *J. Fluid Mech.* 84 (1978) 695–704.
10. P.G. Simpkins and J.E. Godreau, Onset of periodic convection in a vertical slot, AT&T Bell Laboratories Tech. Mem. (unpublished, 1988).